Controlling Photodissociation Pathways via Fano Profiles: NO State Distributions in FNO(S_1) Decomposition

S. A. Reid, J. T. Brandon, and H. Reisler*

Chemistry Department, University of Southern California, Los Angeles, California 90089-0482

Received: October 22, 1992; In Final Form: December 2, 1992

We report coherent control of the NO[v=1,J/v=2,J] ratios obtained following photodissociation in the FNO-(S_1←S_0) (2,0,0) resonance. In FNO dissociation, interference between the simultaneously excited resonance and continuum channels leads to asymmetric absorption line shapes (Fano profiles). The profiles obtained when monitoring NO in v = 1 and v = 2 are different due to different phase shifts associated with the vibrationally adiabatic (v = 2) and nonadiabatic (v = 1) dissociation channels. This leads to variation of the NO[v=1,J/v=2,J] ratios by a factor of ~40 when the dissociation wavelength is changed within the (2,0,0) resonance.

Radiative control of product branching ratios or state distributions in a chemical reaction has long been a goal of photochemistry, and recent work has shown that state and product specificity is possible in favorable cases. A straightforward approach is to access optically an excited state that correlates preferentially with a distinct product channel or internal state (e.g., ClNO(T_1), CH_2IBr).[1,2] Another approach, pioneered by Crim and co-workers, involves vibrationally mediated photodissociation, which results in favorable cases mode and even bond selectivity.[3] However, this type of *mode-selective* control is ultimately limited to systems for which excitation localized on a time scale comparable to that of reaction is possible (i.e., restricted IVR). An alternative approach involves control of branching ratios by the experimenter, exploiting quantum interference effects induced by controlling the phases of the pumping lasers. Several schemes have been proposed, for example, by Brumer and Shapiro,[4] and one of them has been recently implemented by Elliot and co-workers[5] and Gordon and co-workers.[6] In this method, two nanosecond laser pulses having a definite phase relationship are used for simultaneous excitation via differing paths (e.g., one- vs three-photon pumping). Interference between these paths is then controlled by adjusting the phase difference of the two beams. This technique has been successfully used to control the efficiency of a single channel (e.g., photoionization of an atom or a diatomic molecule) but has not yet been extended to multiple channel systems.

In this letter, we report our study of the photodissociation of a triatomic molecule, FNO, and demonstrate coherent control over the vibrational-state distribution of the diatomic fragment by exploiting quantum interference between an unstable resonance in the excited state and the excited-state continuum. Specifically, we show that in the photoinitiated dissociation of FNO on the first excited singlet surface:

$$\mathrm{FNO}(\mathrm{X}^1\mathrm{A}') + h\nu(\nu \sim 33\,000\ \mathrm{cm}^{-1}) \rightarrow \mathrm{FNO}[1^1\mathrm{A}'',(v_1,v_2,v_3)] \quad (1)$$

$$\mathrm{FNO}[1^1\mathrm{A}'',(v_1,v_2,v_3)] \rightarrow \mathrm{NO}\ (\mathrm{X}^2\Pi,v,J) + \mathrm{F}(^2\mathrm{P}) \quad (2)$$

the NO(v=1,J)/NO(v=2,J) ratio can be varied by a factor of ~40 by tuning across a single resonance absorption band. This selectivity derives from the difference in the asymmetric absorption lineshapes obtained when monitoring NO(v=1) and NO(v=2). Such asymmetric absorption line shapes (known also as Fano profiles)[7,8] arise from interference between the simultaneously excited unbound continuum and resonance states. Since a Fano line shape deriving from the interaction between a resonance and a single continuum vanishes at a specific wavelength,[7,8] in principle different product channels can be quenched at wavelengths determined by their Fano profiles (see below).

The first excited state of FNO, $S_1(1^1A'')$, is predominantly repulsive with a shallow well (~400 cm^{-1}) which is separated from the F + NO exit channel by a small barrier lying near the Franck–Condon region.[9] As has been shown by time-dependent 2D calculations, a wave packet initially localized in the Franck–Condon region of FNO(S_1) splits into two parts: one part dissociates directly while the other part is trapped in the well for several vibrational periods. After each vibrational period the wave packet recurs to the Franck–Condon region and again partly leaks to the dissociative continuum.[10] The autocorrelation function describing the time evolution of the wave packet thus exhibits recurrences which in turn lead to the structured absorption spectrum observed experimentally.[9,10] The absorption spectrum consists of an intense progression in the NO stretch (v_1,0,0), and weaker progressions which include bending quanta.[9-12]

In a previous communication, we described how interference between the direct and indirect dissociative paths of FNO(S_1) correlating with a specific NO(v,J) state leads to asymmetric Fano profiles.[12] These profiles were readily observed in the state-specific photofragment yield (PHOFRY) spectra by monitoring different NO(v,J) states and scanning over several resonances in the absorption spectrum. In this report, we turn our attention to the Fano profiles associated with a *single* excited-state resonance but correlating with different NO *vibrational* levels. Specifically, we show that for excitation of the (2,0,0) resonance the different line shapes associated with monitoring NO in v = 2 or v = 1 lead to a large variation of their ratio when scanning across the resonance. To the best of our knowledge, this is the first demonstration that Fano line shapes in photodissociation can be used to control product state distributions.

The experimental arrangement has been described in detail before.[12-14] Briefly, a 5% mixture of FNO in helium was expanded from a pulsed source at stagnation pressures of 500–760 Torr into a vacuum chamber and intersected approximately 15 mm (30 nozzle diameters) from the nozzle orifice by the frequency doubled output (300–320 nm, 2–4 mJ/pulse) of a Nd:Yag laser pumped dye laser system (Quanta-Ray DCR-1/PDL). The resulting NO fragments were detected by laser-induced fluorescence (LIF) on the diagonal sequence of the ($A^2\Sigma^+ \leftarrow X^2\Pi$) transition ($\gamma$ system) by the frequency-doubled output of an excimer laser pumped dye laser system (Lambda Physik EMG201MSC/FL3002), delayed 80–100 ns with respect to the pump pulse. The two laser beams were collinear but counterpropagating with parallel linear polarizations and orthogonal to both the pulsed nozzle and the photomultiplier tube (PMT) used for fluorescence detection.

0022-3654/58/2097-0540$04.00/0

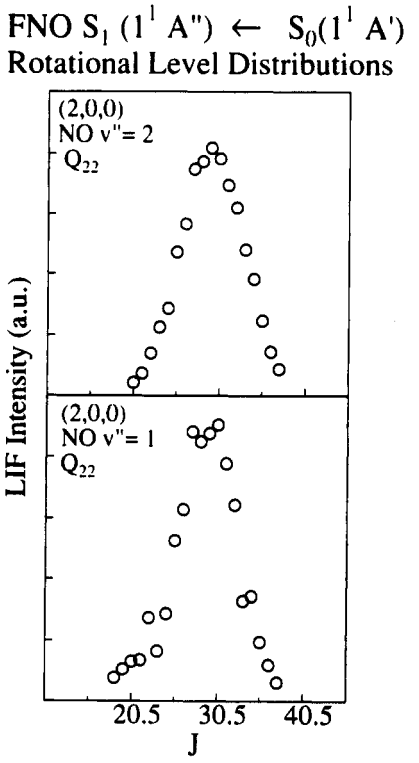

Figure 1. NO rotational state distributions in $v = 2$ (upper panel) and $v = 1$ (lower panel) following excitation in the (2,0,0) band of the FNO (S_1←S_0) transition at 310.96 nm (32 158 cm^{-1}).

Two types of experiments were carried out. In the first arrangement, the photolysis laser frequency was set near the peak of the (2,0,0) resonance at 310.96 nm and the probe laser frequency was scanned over the (1,1) and (2,2) bands of the NO γ system to obtain the rotational state distributions in NO $v = 1$ and 2, respectively. In this arrangement the probe pulse energy was attenuated to ~10 μJ/pulse in a 5.0-mm diameter beam to avoid saturation of the strong NO transitions. In the second arrangement, the probe laser frequency was set to monitor a specific rovibrational level of NO and the photolysis laser frequency was scanned to obtain the PHOFRY spectra in the region of the (2,0,0) band. In this arrangement higher probe pulse energies were used (~10–40 μJ) to minimize shot-to-shot fluctuations. For both arrangements the PMT signal was digitized, stored, and transferred to a personal computer which controlled both data acquisition and laser frequency stepping.

Figure 1 displays the rotational state distributions of the NO fragment for both the vibrationally adiabatic and nonadiabatic channels (i.e., those yielding NO $v = 2$ and 1, respectively) following excitation near the peak of the (2,0,0) band at 310.96 nm (32 158 cm^{-1}). The distribution for the vibrationally adiabatic channel, which is Gaussian in shape and quite narrow (fwhm ~ 10 J), is well fit by a modified rotational reflection model in which the excited-state wave function at the transition state is reflected into the NO rotational distribution, mediated by the exit-channel interactions.[9] The distribution for the vibrationally nonadiabatic channel is very similar, suggesting that the angular dependence of the potential is similar for both channels. Analysis of these distributions yields a vibrational branching ratio [(NO(v=2)/NO(v=1)] = 0.83 ± 0.10 at 32 158 cm^{-1}.

Displayed in Figure 2 are pairs of state-specific PHOFRY spectra taken while monitoring NO in $J = 26.5$ and 29.5 of, respectively, $v = 1$ and $v = 2$. The spectra were obtained by excitation of the Q_{22} transitions in the γ(1,1) and γ(2,2) bands. Note the obvious asymmetry of the (2,0,0) resonances, a phenomenon observed also in the PHOFRY spectra of other monitored NO levels. In each panel, the spectra for $v = 2$ and $v = 1$ are normalized such that their relative intensities at 32 158

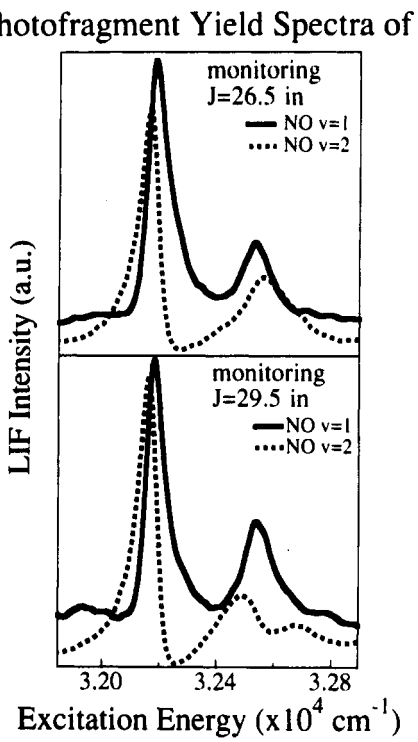

Figure 2. Photofragment yield spectra (PHOFRY) in the region of the FNO [S_1(2,0,0) ← S_0(0,0,0)] transition. The upper panel displays two PHOFRY spectra obtained by monitoring NO(J=26.5) in $v = 1$ and $v = 2$, respectively. Similar spectra for NO(J=29.5) are shown in the lower panel. The spectra in each panel are normalized to the rotational populations displayed in Figure 1.

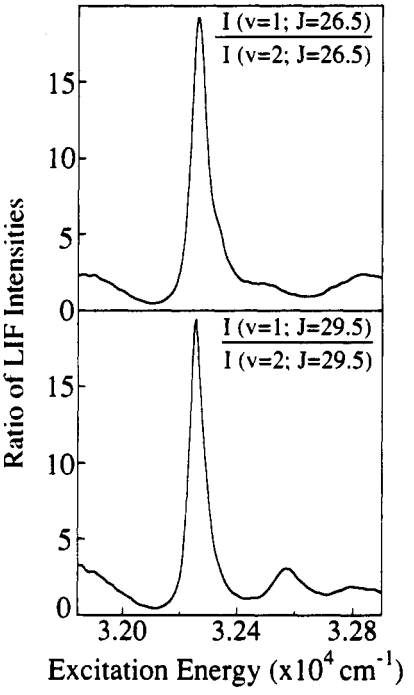

Figure 3. Rotational state specific yield ratios of NO(J) $v = 1$ vs $v = 2$ in the region of the FNO[S_1(2,0,0) ← S_0(0,0,0)] transition, obtained by dividing the smoothed and normalized PHOFRY spectra displayed in Figure 2.

cm^{-1} are equal to the relative rotational populations of the corresponding NO(v,J) levels. In Figure 3 we show the [v=1/v=2] ratios for the monitored rotational levels as a function of excitation wavelength. These curves were obtained by dividing the smoothed curve for $v = 1$ by that for $v = 2$. (The smoothing does not alter the shapes of the curves.) Clearly each ratio varies strongly across the (2,0,0) resonance, particularly in the region 32 200–32 400 cm^{-1}. The [v=1/v=2] ratio in this region varies

from a minimum of ~0.5 to a maximum of 20 when monitoring either $J = 26.5$ or 29.5.

In characterizing the asymmetric line shapes, it is customary to fit them to a Fano line profile:[7]

$$\sigma = \sigma' + \sigma_0(q + \epsilon)^2/(1 + \epsilon^2) \quad (3)$$

where σ_0 is the cross section for direct excitation to the continuum associated with a specific v,J level of NO, σ' is the cross section for excitation of other continua and q is the so-called asymmetry parameter (or shape profile index) given by[7]

$$q = \frac{\langle b|\mu|i\rangle}{\langle c|\mu|i\rangle \pi \langle c|H'|b\rangle} \quad (4)$$

In this equation $|i\rangle$, $|b\rangle$, and $|c\rangle$ are the wave functions for the initial state, bound resonance (modified by the interaction with the continuum), and continuum states, respectively, μ is the transition dipole moment, $\epsilon = (E - E')/(\Gamma/2)$, and $\langle c|H'|b\rangle$ represents the coupling between the bound and continuum states with H' being the interaction Hamiltonian. Since the matrix elements are signed quantities, q can be positive or negative. Also, note that when only one continuum participates, the cross-section vanishes when $q = -\epsilon$. In the case of the FNO, we have shown that many lineshapes can be well fit by eq 1.[12]

In the absence of spectral overlap, the shapes of the Fano profiles in the region of the (2,0,0) resonance do not change markedly (i.e., similar q and Γ) when different NO J levels are monitored *within the same vibrational level*. The line profiles change, however, when monitoring the vibrationally adiabatic versus the nonadiabatic channel. The Fano fits show that the width parameter Γ stays the same at 70 ± 20 cm^{-1} for both vibrational levels, but q changes sign, although it is also of comparable magnitude (i.e., $q = \pm 5 \pm 2$). As a consequence, the cross sections for these two channels should vanish at *opposite* sides of the (2,0,0) resonance maximum. This behavior leads to a fast change in the $[v=1/v=2]$ ratio in the 32 200–32 400 cm^{-1} wavelength region, as depicted in Figure 3. The peak in this ratio corresponds to the wavelength where the $v = 2$ cross section almost vanishes. In principle, we expect a second region of selectivity where the $v = 1$ cross section should have gone to zero (i.e., at ~32 100 cm^{-1}); however, owing to overlap with the (1,0,3) resonance,[12] this is not the case, and the selectivity is reduced. Although we present here vibrational branching ratios for only two pairs of (v,J) levels, these rotational levels are at the peak of the $v = 1$ and 2 rotational distributions (Figure 1). Moreover, traces taken by monitoring J levels between 22.5 and 41.5 in $v = 1$ show similar Fano profiles that can be fit with similar q and Γ parameters within experimental uncertainty. Thus, the state selectivity demonstrated in Figure 3 for specific NO(v,J) levels represents selectivity in the total $[v=1/v=2]$ ratio.

To gain physical insight into the origin of the line shapes, an alternative but equivalent representation involving the relative phase shifts and their variation with excitation wavelength can be invoked. In such a picture, which is widely used in scattering theory,[15] the partial absorption cross-sections are given in terms of the resonant, η_R, and continuum, η_C, phase shifts:[8]

$$\sigma(E) \propto \sin^2(\eta_R + \eta_C) \quad (5)$$

where

$$\eta_R = -\arctan\left[\frac{\pi|V_{E'}|^2}{E - E'}\right] = -\arctan \epsilon \quad (6)$$

and E' is the resonance position. The resonant phase shift, η_R, varies sharply across the resonance (i.e., by π),[15] causing sharp variations of the excitation probability, while η_C varies very slowly in the region of the resonance. When the continuum and resonance are excited simultaneously and only one continuum is involved, the interference causes the transition probability to vanish on one side of the resonance at excitation energy $E = E_0$, such that $\eta_{R0} + \eta_C = 0$ and[7,8]

$$\tan \eta_0 = -\frac{E_0 - E'}{\pi|V_{E_0}|^2} = -\frac{E_0 - E'}{\Gamma/2} \quad (7)$$

Thus, the relative phase-shifts and their variations with wavelength determine the shape of the absorption line.

Our results demonstrate that a large change in phase shift between the vibrationally adiabatic and nonadiabatic channels can lead to control of their ratio and that coherence can be preserved even in nonadiabatic channels. We point out that in fact neither channel is truly adiabatic as both require some degree of vibrational–translational (V–T) coupling. This is a result of the mismatch between the NO stretch vibration in FNO (~1000 cm^{-1}) and free NO (~1800 cm^{-1}), which necessitates some energy redistribution in each channel. The similarity of the $v = 2$ and 1 *rotational* distributions indicates that V–T energy transfer is the predominant coupling mechanism in both the vibrationally adiabatic and nonadiabatic channels, but the amount of energy transfer is different. This may account qualitatively for the different phase shifts involved in the two pathways. The comparable yields of NO $v = 2$ and $v = 1$ near the peak of the resonance indicate that both pathways are equally likely, and it is intriguing that both involve a similar Γ, the effective resonance width. The preservation of coherence despite the exit-channel couplings may be a result of the small degree of mode-mixing in FNO(S_1) dissociation. For example, we have shown that the S_1 bending mode is not coupled significantly to the other degrees of freedom and is mapped into product rotation.[9] It is this weak V–R coupling of the stretching motion, evidenced by the marked similarity of the rotational distributions, that prevents the destruction of coherence from the numerous accessible rotational channels. It is likely that even though some degree of V–T coupling must accompany the evolution of the NO stretch vibration, only a small region of phase space is sampled, with the resulting preservation of coherence.

The preliminary results described here represent a first example of control of a branching ratio in photodissociation via interferences in the absorption cross-sections (Fano line shapes). At this point the effect has been observed for a single FNO($S_1 \leftarrow S_0$) resonance, (2,0,0), and the observations have not yet been described by rigorous theory. Clearly, additional results on different S_1 resonances are desirable, as well as a theoretical description of these intriguing observations.

Acknowledgment. The authors wish to thank Amy Ogai for assistance in obtaining and analyzing the NO rotational distributions and Stas Ionov for careful reading of the manuscript. This work is supported by NSF under Grants CHE9023632 and CHE9104248.

References and Notes

(1) Qian, C. X. W.; Ogai, A.; Brandon, J. T.; Bai, Y. Y.; Reisler, H. *J. Phys. Chem.* **1991**, *95*, 6763.

(2) Butler, L. F.; Hintsa, E. J.; Shane, S. F.; Lee, Y. T. *J. Chem. Phys.* **1987**, *86*, 2051.

(3) Crim, F. F.; Hsaio, M. C.; Scott, J. L.; Sinha, A.; Vander Wal, R. L. *Philos. Trans. R. Soc. London A* **1990**, *332*, 259.

(4) Brumer, P.; Shapiro, M. *Acc. Chem. Res.* **1989**, *22*, 407.

(5) (a) Chen, C.; Yin, Y.-Y.; Elliot, D. S. *Phys. Rev. Lett.* **1990**, *64*, 507. (b) Chen, C.; Elliot, D. S. *Phys. Rev. Lett.* **1990**, *65*, 1737.

(6) Li, S.-P.; Park, S. M.; Xie, Y.; Gordon, R. J. *J. Chem. Phys.* **1992**, *96*, 6613.

(7) (a) Fano, U. *Phys. Rev.* **1961**, *124*, 1866. (b) Lefebrve-Brion, H.; Field, R. W. *Perturbations in the Spectra of Diatomic Molecules*; Academic: Orlando, 1986; pp 331–412.

(8) Massey, H. S. W.; Burhop, E. H. S.; Gilbody, H. B. *Electronic and Ionic Impact Phenomena*, 2nd ed.; Oxford University Press: London, 1969; Vol. 1, pp 594–664.

(9) Ogai, A.; Brandon, J.; Reisler, H.; Suter, H. U.; Huber, J. R.; von Dirke, M.; Schinke, R. *J. Chem. Phys.* **1992**, *96*, 6643.

(10) Suter, H. U.; Huber, J. R.; von Dirke, M.; Untch, A.; Schinke, R. *J. Chem. Phys.* **1992**, *96*, 6727.

(11) We use normal-mode notations even though the peaks correspond to unstable resonances.

(12) Brandon, J. T.; Reid, S. A.; Robie, D. C.; Reisler, H. *J. Chem. Phys.* **1992**, *97*, 5246.

(13) Qian, C. X. W.; Ogai, A.; Iwata, L.; Reisler, H. *J. Chem. Phys.* **1990**, *92*, 4296.

(14) Ogai, A.; Qian, C. X. W.; Reisler, H. *J. Chem. Phys.* **1990**, *93*, 1107.

(15) Joachain, C. J. *Quantum Collision Theory*; North-Holland: Amsterdam, 1975.